# APPENDIX A

## Application of FT-IR Emission/Transmission (E/T) Spectroscopy to Study Coal Combustion Phenomena

Revised 7/88

# APPLICATION OF FT-IR EMISSION/TRANSMISSION (E/T) SPECTROSCOPY TO STUDY COAL COMBUSTION PHENOMENA

P.R. Solomon, P.L. Chien, R.M. Carangelo, P.E. Best*, and J.R. Markham
Advanced Fuel Research, Inc., 87 Church Street, East Hartford, CT 06108

## ABSTRACT

This paper describes the application of a recently described Fourier Transform Infrared (FT-IR) Emission and Transmission (E/T) technique to study coal flames produced in a transparent wall reactor. Comparisons are made for the ignition, soot formation, particle temperature and gas temperature for a number of coals varying in rank from lignite to low volatile bituminous. Samples of chars prepared at different temperatures and demineralized coals were also studied. Flame properties were compared with characteristics of the samples to determine the factors which control flame behavior. A comparison of the ignition of several samples suggests that the rate of ignition correlates with the initial rate of weight loss in air in a TGA experiment at lower temperatures. Ignition of chars is heterogeneous; ignition of high rank coals is homogeneous; but low rank coals exhibit both homogeneous and heterogeneous contributions to ignition. Soot formation in combustion correlates well with tar yield in pyrolysis suggesting that tar is the chief precursor of soot. A new ignition phenomenon has been observed in which char particles already ignited make a transition to a more intense burning mode.

# APPLICATION OF FT-IR EMISSION/TRANSMISSION (E/T) SPECTROSCOPY TO STUDY COAL COMBUSTION PHENOMENA

P.R. Solomon, P.L. Chien, R.M. Carangelo, P.E. Best*, and J.R. Markham
Advanced Fuel Research, Inc., 87 Church Street, East Hartford, CT 06108 USA

## INTRODUCTION

Better understanding of the coal combustion process would promote more reliable utilization of coals having a diversity of characteristics and would enable improved combustion systems to be designed and developed. Many aspects of coal combustion are understood and can be adequately modeled. However, several unresolved fundamental issues remain: ignition, soot formation, swelling, char reactivity, ash formation and the influence of turbulence on chemical reactions and particle dispersion.

Techniques to measure these phenomena must be capable of following the behavior of the solid particles as well as the gas species. Many of the techniques for gas analysis have been recently reviewed.[1] For particle temperature, 2 or more color pyrometry has been used extensively.[2-6] Advances in optical emission techniques to measure simultaneously size, velocity, and temperature of single particles have also been reported.[7,8]

Recently, Fourier Transform Infrared (FT-IR) Spectroscopy has shown promise as a versatile technique. FT-IR transmission spectroscopy has been used as an in-situ diagnostic technique to determine both gas concentrations[9] and temperatures.[10,11] An FT-IR emission and transmission (E/T) spectroscopic technique has been applied to particles, gases and soot in flames.[12-15] The E/T technique has been used previously for gases and soot.[5,16-18]

*Permanent address: Physics Depart., University of Connecticut, Storrs, CT 06268

Advantages of the technique include: i) the capability to determine separate temperatures and concentrations for individual gas species as well as for solid particles by employing different regions of the infrared spectrum; ii) the capability to determine temperatures as low as 100°C and consequently the ability to follow particle temperatures prior to ignition; iii) the ability to make measurements in densely loaded streams to study cloud effects (in this respect, the technique is a good complement to the single particle measurements[7,8]); iv) the capability to separate the radiative contribution from soot and from char particles; and v) the capability to measure particle sizes. The disadvantage of FT-IR E/T spectroscopy is that the measurements are for an ensemble of particles over a line-of-sight, and tomographic techniques must be used to obtain spatially resolved data.

This paper describes the application of the FT-IR E/T technique to study coal flames produced in a transparent wall reactor. Comparisons are made for the ignition, soot formation, particle temperature and gas temperature for a number of coals varying in rank from lignite to low volatile bituminous. Samples of chars prepared at different temperatures and demineralized coals were also studied.

## EXPERIMENTAL

**Apparatus** - The Transparent Wall Reactor (TWR) facility shown in Fig. 1 consists of an electrically heated furnace and a heat exchanger. Dry air is passed through the heat exchanger and exits the top of the furnace through a screen to smooth the flow. The hot gas stream, which is 10 cm in diameter, remains relatively hot and undisturbed for approximately 20 cm above the screen. Coal entrained in a cold carrier gas (dry air) is injected through a co-axial 4 mm diameter tube.

The feed rates for the carrier gas and the hot gas were 225 ml/min and 173 l/min, respectively. The hot gas exits the screen at a temperature of 850°C and a

velocity of 2.8 m/sec. Short exposure photographs show particle tracks which indicate that the coal particles are moving at about 2.5 m/sec near the injector and 4.8 m/sec in the flame.

An octagonal glass enclosure shields the reacting stream from room air currents. The enclosure has movable KBr windows to allow access to the flame by the FT-IR spectrometer (a modified Nicolet 20SX). The spatial resolution is approximately 5 mm. As discussed in Ref. 14, emission measurements are made with a movable mirror placed in the beam to divert the beam to the emission detector. Transmission measurements are made with the movable mirror out of the beam. A flow of air along the inside of the enclosure keeps the glass from overheating.

There is absorption from the $CO_2$ and $H_2O$ in the sheath air and from air along the optical path as well. This is accounted for since the transmittance is the ratio of a spectrum taken in the presence of a sample (and the interfering species) to a background spectrum (which includes the interfering species). It is accounted for in the emission spectrum since the path correction obtained using a black-body reference includes these interferences. Figure 2 shows photographs of three flames: a) a lignite which ignites close to the nozzle, b) a low volatile bituminous coal which ignites (apparently homogeneously in the gas phase) higher up, and c) a close up of a high volatile bituminous coal flame showing volatile flames which are much larger than the particles they surround. Such volatile flames have been observed previously.[19,20]

Samples - The samples used in these experiments were sieved fractions of a lignite, a subbituminous coal, and several bituminous coals. Samples have been demineralized by the Bishop and Ward technique.[21] Chars were prepared from some of the coals in nitrogen in a previously described entrained flow reactor.[10,20] The characteristics of the coals have been previously published.[22-25] Table I summarizes the coals, preparation procedures, and references to the previously published data. The samples were also characterized in a TGA to determine their weight loss at constant heating rate in nitrogen (to determine the volatile

content) and in air (to provide a relative measure of the samples' reactivity[24,25] and the ash concentration).

## ANALYSIS

For multi-phase reacting systems, measurements are made of the transmittance and the radiance, and from these a quantity called the normalized radiance is calculated. The analysis, which follows Siegel and Howell[26] has been presented previously.[12] The relevant equations for a homogeneous medium are presented below.

**Transmittance, $\tau_\nu$** - For a medium containing gases and soot with absorption coefficients $\alpha_\nu^g$ and $\alpha_\nu^s$ and particles of geometrical cross sections area A at a density of N particles $cm^{-3}$, the transmittance, $\tau_\nu$ is given by

$$\tau_\nu = \exp(-(\alpha_\nu^s + \alpha_\nu^g + NAF_\nu^t)\, L) \tag{1}$$

where $F_\nu^t$ is the ratio of the total cross section (extinction) to geometric cross section, and L is the path length. $\tau_\nu$ is sometimes plotted as a percentage.

**Normalized Radiance, $R_\nu^n$** - The normalized radiance, $R_\nu^n$, which is defined as the radiance divided by $(1-\tau_\nu)$ is given by,

$$R_\nu^n = \frac{\alpha_\nu^s R_\nu^b(T_s) + \alpha_\nu^g R_\nu^b(T_g) + NA\, \epsilon_\nu\, R_\nu^b(T_p) + NAF_\nu^{s'} R_\nu^b(T_w)}{\alpha_\nu^s + \alpha_\nu^g + NAF_\nu^t} \tag{2}$$

where $R_\nu^b(T_g)$, $R_\nu^b(T_s)$, $R_\nu^b(T_p)$, and $R_\nu^b(T_w)$ are the black-body emission spectra at the temperatures $T_g$, $T_s$, $T_p$, and $T_w$ of the gas, soot, particle, and wall, respectively. $\epsilon_\nu$ is the particle's spectral emittance and $F_\nu^{s'}$ is the cross section for scattering radiation into the spectrometer. In Eq. 2, zero scattering is assumed for soot particles in the IR region. For the geometry of the TWR scattering from particles, $F_\nu^{s'}$ may be neglected, since $T_w$ is room temperature. Temperature measurements appear to be accurate to $\pm$ 50°C.

## RESULTS

**FT-IR E/T Measurements in Coal Flames** - Results have been obtained for a series of samples including coal, demineralized coal, and char. FT-IR measurements were made along the center of the flame at several positions above the coal injector. It is recognized that the flame is not spatially homogeneous along the line-of-sight. In this case, application of the analysis yields the average properties along a line-of-sight. Work is currently in progress to develop tomographic methods to obtain spatially resolved data.

Figure 3 presents transmittance and normalized radiance spectra obtained for a Rosebud subbituminous coal flame at several distances above the nozzle: 5 cm above the nozzle is in the region prior to ignition; 9 cm is at the beginning of the ignition region; 11 cm is in the ignition region; 13 cm and 14 cm are in the brightest part of the flame; and 17, 20, and 25 cm are where burnout occurs.

Figure 3c presents the transmittance spectra as 100-% transmittance. In the optically thin limit, the amplitude of (100-% transmittance) is proportional to the intersected surface area of the particles, NAL, times the extinction efficiency, $F_\nu^t$, where $F_\nu^t = 1$ in the absence of diffraction. The attenuation at 5 cm is almost entirely from coal particles. The spectrum slopes due to diffraction effects, and the shape of $\tau_\nu$ which is proportional to $F_\nu^t$, may be used to determine particle size. A technique which obtains the mean particle radius and spread of a Gaussian distribution of particle sizes from the transmittance has been demonstrated.[15]

At 9 cm, a few particles have ignited and attenuation from $CO_2$ can be seen. At 11 cm, the attenuation is flatter due to the appearance of soot. The soot attenuation slopes downward toward low frequencies (0 $cm^{-1}$), the particle attenuation slopes upward toward low frequencies, and the sum appears flat. The attenuation at 11 cm and at 13 cm, contains larger contribution for $CO_2$ and $H_2O$, a contribution from soot, as well as a contribution from the particles. To resolve the spectrum into particle and soot contributions, $F_\nu^t$ for the particles is assumed

to have the same shape as prior to ignition, and the particle transmittance is assumed to be equal to the measured transmittance extrapolated to 0 $cm^{-1}$ (where the attenuation from soot goes to zero). A straight line extrapolation is made below 3500 $cm^{-1}$ excluding the region of the spectrum containing $CO_2$ and $H_2O$ bands. The estimated uncertainty in the extrapolation is $\pm$ 10% of the transmittance. The soot contribution is the difference between the particle attenuation and the total as shown in Fig. 3c (11 cm). Much larger soot contributions were observed for bituminous coals. Above the ignition region, at 14, 17, 20, and 25 cm, (100-% transmittance) progressively reduces as the particles burn out. The 17, 20, and 25 cm cases show the presence of ash (the dips near 1200 $cm^{-1}$ due to the Christiansen effect). Such dips which are observed near strong absorption bands, are due to reduced scattering as the material's index of refraction more closely matches that of the surrounding medium. Dips in this region have previously been observed for coal ash and small silica spheres.[15]

The normalized radiance measurements are shown in Fig. 3b and Fig. 3a on an expanded scale for the 5, 9, 20, and 25 cm cases. The average temperatures are obtained by comparing the normalized radiance to theoretical black-body curves. Prior to ignition (5 cm), a particle temperature of 575 K is determined from the region between 1200 and 1600 $cm^{-1}$ where for coal (which is non-gray[12,13,15,27]) $\epsilon \approx 1$. At 9 cm, the presence of radiation intensity above 4000 $cm^{-1}$ in the spectra shows that a few particles have ignited. The combination of ignited and unignited particles is fit theoretically assuming that there are two classes of particles; very hot burning char particles and moderate temperature coal particles. The spectra for the two classes are added to provide a fit to the observed spectrum. The temperature of the ignited particles (1950 K) is determined from the shape of the region above 4000 $cm^{-1}$ (where the contribution from the unignited particles is negligible) assuming a gray-body ($\epsilon = 0.8$) for char.[12,13,15] The spectrum is fit using a black-body multiplier of 0.043. The black-body multiplier, M, is the constant fraction of the theoretical black-body which produces the best match in

shape and amplitude to the experimental data. For a completely homogeneous sample of gray-body particles, M would be the particle's emissivity. For the case considered here, some particles may be unignited, or ash particles may be present at a much lower temperature than the coal particles and have a very low emittance. Then, M is approximately the fraction of particles in each category times their emissivity.

Assuming an emissivity of 0.8 for char and fitting the high frequency end of the spectrum indicates that 5.4% of the particles are ignited. The temperature of the ignited particles is about 750°C higher than the preheated gas stream. This is in reasonable agreement with the measurements of Timothy et al.[2] and with the diffusion burning limit calculated by Waters et al.[28] and Timothy et al.[2]

The contribution from unignited particles are fit by adding a gray-body spectrum ($\epsilon = 0.9$) for the remaining particles (94.6%). The temperature of the unignited particles are fit to match the region below 1600 $cm^{-1}$ where coal has an emissivity near 0.9.[13,15]

In the region where many particles (11 cm), and then most particles (13 cm) are ignited, the shape of the spectrum is consistent with a temperature of 2010 K and 1900 K, respectively. The particle temperature increase over the 9 cm case is thought to be due to the effect of cloud burning i.e., the increase in the ambient gas temperature due to heat released by the neighboring coal particles.

A value of M of 0.32 at 11 cm is consistent with only partial ignition of the particles and of 0.85 at 13 cm with complete ignition and a value of $\epsilon = 0.7$ to 0.9 for char.[12,13,15] In the upper part of the flame, the particle contributions to the radiance becomes progressively lower as the particles burn out, leaving fly ash

The $CO_2$ temperatures can be obtained from the normalized radiance, as well. In Fig. 3, a rough estimate of the $CO_2$ temperature was made by fitting a black-body to the $CO_2$ amplitude in the normalized radiance. This approximation is reasonably accurate when the $CO_2$ bands are large compared to the soot or particle contribution to the spectrum. For the most accurate determination of gas temperatures by the E/T technique the gas emission and transmission lines should be

corrected for the presence of soot or particles. This was done for the $CO_2$ temperatures presented in Fig. 4. Comparison of Figs. 3 and 4 indicates that the method of laying black-body temperature curves over the total spectra, without correcting for particles or soot, contributes errors of the order of 100°C in the present case.

The results of Fig. 3 are summarized in Fig. 4. Figure 4 also includes an estimate of the particles' residence time based on photographic measurements of their velocity. Figure 4b presents the particle and $CO_2$ temperatures and M and Fig. 4a presents the soot, $CO_2$ and particles contributions to the infrared absorption as a function of distance above the nozzle. The magnitude of these absorptions are related to the respective concentrations. Prior to ignition, the temperatures, $CO_2$ and soot absorptions, and the values of M for ignited particles are low. At ignition, the $CO_2$ and particle temperatures and the $CO_2$ and soot absorptions go up sharply. In the region where there is soot, the particle temperature is an average of both char and soot temperatures. The influence of the soot temperature on the particle temperature has been analyzed by Grosshandler.[29] In this region, M increases to over 0.8. After ignition, the particle and soot absorptions both fall rapidly as they oxidize. M falls as the ash fraction increases. For the emission at 25 cm, (Fig. 3a) a strong contribution can be seen in the radiance near 1000 $cm^{-1}$ from the ash. As for the 9 cm case, a sum of two particle classes is used to fit the data; ignited char and ash. In this case, the ash is assumed to be at the gas temperature (1440 K) and to have zero emissivity above 4000 $cm^{-1}$. The sum spectrum then determines the emissivity ($\epsilon$ = 0.55) near 1000 $cm^{-1}$. This is in reasonable agreement with previous measurements for coal ash.[30]

**A Correlation of Flame Properties with Sample Characteristics** - Several flame characteristics which varied with sample properties were examined to determine what sample properties were the controlling factors and why. A comparison of the $CO_2$ absorbance profiles, which is a by-product of the ignition behavior, is presented

in Fig. 5a, for the raw and demineralized Rosebud coal, and Rosebud chars produced at 900°C and 1500°C. Ignition for the coals is accompanied by a more rapid increase in $CO_2$ absorbance than seen for the chars. This is believed to be due to the rapid release of energy from the combustion of volatiles. The position of the ignition also varies for the four samples.

To determine what controls the ignition, measurements have been made of the weight loss of coal in a TGA, both under inert and oxidizing conditions. The objective is to correlate what happens in the TGA at temperatures from 450°C to 600°C to what happens during ignition in the TWR at similar particle temperatures. As shown in Fig. 5b, the ignition distance correlates well with the temperature for 10% weight loss in air measured at a constant heating rate of 30°C/min in a TGA. The lower the temperature to achieve 10% weight loss in the TGA, the shorter the ignition distance in the TWR.

To provide additional information on what produces the 10% weight loss, measurements on identical samples were made in the TGA for inert gas (nitrogen) and the weight loss compared to that in air. In the case of the previously formed chars, the TGA weight loss in air is almost exclusively due to char oxidation since there is no corresponding weight loss in nitrogen and hence, the ignition in the TWR must be heterogeneous (i.e., oxidation within the porous solid matrix). For high rank coals, the first 10% weight loss in the TGA under oxidizing conditions is almost the same as in nitrogen and so is mostly due to pyrolysis, consistent with homogeneous ignition in the TWR. For low rank coals, however, there is a significant early weight loss in the TGA in air due to heterogeneous oxidation, and it appears that there is a significant heterogeneous contribution to the ignition in the TWR. This is consistent with the observation that the demineralized Rosebud coal (which is less reactive to oxidation than the raw coal) is more difficult to ignite (Fig. 5a). The results are also consistent with the measurements of Midkiff et al.[31] who conclude that there is a significant weight loss due to heterogeneous oxidation in combustion for low rank coals.

A comparison of the soot concentration for 3 samples is shown in Fig. 5c. The demineralized Rosebud produces about twice the soot as the raw sample, and the char produces almost none. As shown in Fig. 5d, the soot production correlates well with the yield of tar as determined in pyrolysis experiments. Pyrolysis was performed in an entrained flow reactor described previously.[10,22] The higher the tar yield, the higher the soot yield. The relationship between tar and soot is consistent with the results of Wornat et al.[32] and Nenniger et al.[33]

Based on previous infrared measurements of soot in which the complex index of refraction of Dalzell and Sarofim[34] was used to relate the infrared attenuation to the volume fraction[14], the mass of soot in the line-of-sight was calculated and compared with the mass of coal in the same volume. A maximum value of 1.2% of the Rosebud mass appeared as soot at any point along the flame. Performing the same calculation for the other coals, it appears that no more than 1/3 of the tar appears as soot at any one point. This is not unreasonable considering that soot is simultaneously being formed and consumed by oxidation.

Figure 5e compares the value of M for ignited particles, for the raw coal, the demineralized coal and the 900°C char. M can be less than 1.0 due to unignited particles and/or a low value of emissivity. Prior to ignition, all three samples have low values of M due to unignited particles. At ignition, M for the two coals goes up rapidly as the particles ignite and soot is formed. Above the ignition region, where all the particles are expected to be ignited, M drops rapidly for the raw coal but remains high for the demineralized coal. The source for this effect appears to be ash particles which are shed from the burning char particles. The ash particles that are shed will increase (100-% transmittance) without adding significantly to the radiance because of their low temperature and low emissivity. TGA analysis of the captured samples of char early in the flame showed that a significant fraction of the minerals (30%) had already been shed.

An alternative explanation is that the unshed ash particles act as diffuse scatterers which lowers the emissivity. However, a direct measurement of the

emissivity of captured char particles using the E/T technique[13] at a lower temperature (800°C), shows the emissivity to be approximately 0.85, suggesting that the reduction of the emissivity due to surface ash is not important.

Figure 5f presents a correlation between M above ignition (where all particles should be ignited and the soot has been consumed) with the ash content of the coal. The higher the ash content, the lower M, in agreement with either hypotheses.

## CONCLUSIONS

1. The FT-IR E/T technique is a versatile technique for coal combustion diagnostics allowing measurements of particle concentrations and temperatures and gas compositions, concentrations, and temperatures.
2. A comparison of the ignition of several samples suggests that the rate of ignition correlates with the initial rate of weight loss in air in a TGA experiment at lower temperatures. Comparison of the TGA weight loss in air with that in nitrogen suggest that ignition of chars is heterogeneous; ignition of high rank coals is homogeneous; but low rank coals exhibit both homogeneous and heterogeneous contributions to ignition.
3. Soot formation in combustion correlates well with tar yield in pyrolysis suggesting that tar is the chief precursor of soot.

## ACKNOWLEDGEMENT

This work was supported under the U.S. Department of Energy contracts #DE-AC21-85MC22050 and #DE-AC21-86MC23075 and NSF Grant No. CBT-8420911.

## REFERENCES


1. Penner, S.S., Wang, C.P., and Bahadori, M.Y.: Twentieth Symposium (International) on Combustion, p. 1149, The Combustion Institute, (1984).
2. Timothy, L.D., Sarofim, A.F., and Beer, J.M.: Nineteenth Symposium (International) on Combustion, p. 1123, The Combustion Institute, (1982).
3. Mitchell, R.E. and McLean, W.J.: Nineteenth Symposium (International) on Combustion, p. 1113, The Combustion Institute, (1982).
4. Cashdollar, K.L. and Hertzberg, M.: Combustion and Flame 51, 23, (1983).
5. Altenkirch, R.A., Mackowski, D.W., Peck, R.E., and Tong, T.W.: Comb. Sci. Tech. 41, 327, (1984).
6. Seeker, W.R., Samuelsen, G.S., Heap, M.P., and Trolinger, J.D.: Eighteenth Symposium (International) on Combustion, p. 1213, The Combustion Institute, (1981).
7. Macek, A. and Bulik, C.: Twentieth Symposium (International) on Combustion, p. 1223, The Combustion Institute, (1984).
8. Tichenor, D.A., Mitchell, R.E., Hencken, K.R., and Niksa, S.: Twentieth Symposium (International) on Combustion, p. 1213, The Combustion Institute, (1984).
9. Solomon, P.R., Hamblen, D.G., and Carangelo, R.M.: in Fuel Science, ACS Symp. Series 205, 4, 77, (1982).
10. Solomon, P.R., Hamblen, D.G., Carangelo, R.M., and Krause, J.L.: Nineteenth Symposium (International), p. 1139, The Combustion Institute, (1982).
11. Ottensen, D.K. and Stephenson, D.A.: Combustion and Flame 46, 95, (1982).
12. Best, P.E., Carangelo, R.M., and Solomon, P.R.: Combustion and Flame 66, 47, (1986).
13. Solomon, P.R., Carangelo, R.M., Best, P.E., Markham, J.R., and Hamblen, D.G.: Twenty-first Symposium (International) on Combustion, p. 437, The Combustion Institute, (1987).

14. Solomon, P.R., Best, P.E., Carangelo, R.M., Markham, J.R., Chien, P.L., Santoro, R.J., and Semerjian, H.G.: Twenty-first Symposium (International) on Combustion, p. 1763, The Combustion Institute, (1987).

15. Solomon, P.R., Carangelo, R.M., Best, P.E., Markham, J.R., and Hamblen, D.G.: Fuel **66**, 897, (1987).

16. Tourin, R.H.: Spectroscopic Gas Temperature Measurement, Elsevier, NY, (1966).

17. Limbaugh, C.C.: Infrared Methods for Gaseous Measurement: Theory and Practice, (J. Wormhoudt, Ed.), Marcell Dekker, NY, (1985).

18. Vervisch, P. and Coppalle, A.: Combustion and Flame **52**, 127, (1983).

19. McLean, W.J., Hardesty, D.R. and Pohl, J.H., Eighteenth Symposium (International) on Combustion, The Combustion Institute, 1239, (1981).

20. Timothy, L.D., Froelich, D., Sarofim, A.F., and Beer, J.M.: Twenty-first Symposium (International) on Combustion, p. 1141, The Combustion Institute, (1987).

21. Bishop, M. and Ward, D.L.: Fuel **37**, 191, (1958).

22. Serio, M.A., Hamblen, D.G., Markham, J.R., and Solomon, P.R.: Energy and Fuel **1**, 138, (1987).

23. Vorres, K.S.: ACS Div. of Fuel Chem. Preprints **32**, (4), 221, (1987).

24. Best, P.E., Solomon, P.R., Serio, M.A., Suuberg, E.M., Mott, W.R., Jr., and Bassilakis, R.: ACS Div. of Fuel Chem. Preprints **32**, (4), 138, (1987).

25. Solomon, P.R., Serio, M.A., and Heninger, S.G.: ACS Div. of Fuel Chem. Preprints **31**, (2), 200, (1986).

26. Siegel, R. and Howell, J.R., Thermal Radiation Heat Transfer, (Section 20-5), McGraw Hill, NY, (1972).

27. Fletcher, T.H., Baxter, L.L., and Ottesen, D.K.: ACS Div. of Fuel Chem. Preprints **32**, (3), 42, (1987).

28. Waters, B.J., Mitchell, R.E., Squires, R.G., and Laurendeau, N.M.: ACS Div. of Fuel Chem. Preprints **31**, (1), 12, (1986).

29. Grosshandler, W.L.: Combustion and Flame 55, 59, (1984).

30. Solomon, P.R., Hamblen, D.G., Markham, J.R., and Carangelo, R.M.: "Novel Diagnostics for Particulate Properties in Combustion", U.S. US DOE Final Report Contract No. DE-AC01-85ER80313, (1986).

31. Midkiff, K.C., Altenkirch, R.A., and Peck, R.E.: Combustion and Flame 64, 253, (1986).

32. Wornat, M.J., Sarofim, A.F., and Longwell, J.P.: Energy and Fuels 1, (5), 431, (1987).

33. Nenniger, R.D., Howard, J.B., and Sarofim, A.F. Proceedings of the 1983 Int. Conf. on Coal Sci., p. 521, Pittsburgh, PA, (Aug. 15-19, 1983).

34. Dalzell, W.H. and Sarofim, A.F.: J. Heat Transfer 91, 100, (1969).

TABLE 1

SAMPLE CHARACTERISTICS

| Sample | Sample Abbreviation in Figures | Classification or Preparation Conditions[a] | Nominal Particle size (μm) | TGA Analysis | | | | Sample Ref. |
|---|---|---|---|---|---|---|---|---|
| | | | | % Ash[**] | % DAF Volatile[***] Matter | $T_{cr}$(°C)[****] | $T_{10\%}$ Weight loss[**] (°C) | |
| Zap | Z | North Dakota Lignite, Dry | 45-75 | 7.3 | 43.5 | 434 | 360 | (33) |
| Zap 900°C Char | ZC 900 | EFR Pyrolysis, 1 m/s 900°C, 66 cm, in $N_2$ | 45-75 | 12.7 | 22.0 | 418 | 388 | (33) |
| Zap 1500°C Char | ZC 1500 | EFR Pyrolysis, 1 m/s 1500°C, 66 cm, in $N_2$ | 45-75 | 14.3 | 8.8 | 494 | 458 | (33) |
| Argonne Zap | AZ | North Dakota Lignite, Dry | 45-75 | 8.2 | 40.5 | 418 | 335 | (34) |
| Zap Demineralized | DZ | HCl, HF washings, Dry | 45-75 | 0.5 | 44.7 | 550 | 383 | (36) |
| Rosebud | R | Subbituminous Coal, Dry | 45-75 | 15.1 | 42.8 | 485 | 400 | (33) |
| Rosebud 900°C Char | RC 900 | EFR Pyrolysis, 1 m/s 900°C, 66 cm, in $N_2$ | 45-75 | 23.5 | 19.1 | 443 | 440 | (33) |
| Rosebud 1500°C Char | RC 1500 | EFR Pyrolysis, 1 m/s 1500°C, 66 cm, in $N_2$ | 45-75 | 23.4 | 2.6 | 545 | 575 | (33) |
| Rosebud Demineralized | DR | HCl, HF washings, Dry | 45-75 | 3.7 | 39.1 | 500 | 432 | (36) |
| Argonne Pittsburgh | Pit | Bituminous coal (HVAB) | 45-75 | 3.2 | 37.2 | 600 | 488 | (34) |
| Argonne Pocahontas | P | Bituminous coal (LVB) | 45-75 | 5.1 | 20.0 | 528 | 512 | (34) |

[a] EFR - Entrained Flow Reactor
[**] TGA analysis in air at 30 K/min to 900°C
[***] TGA Analysis in $N_2$ at 30 K/min to 900°C
[****] TGA analysis in $N_2$ at 30 K/min to 900°C followed by in air at 30 K/min to 900°C; critical temperature defined in (35,36).

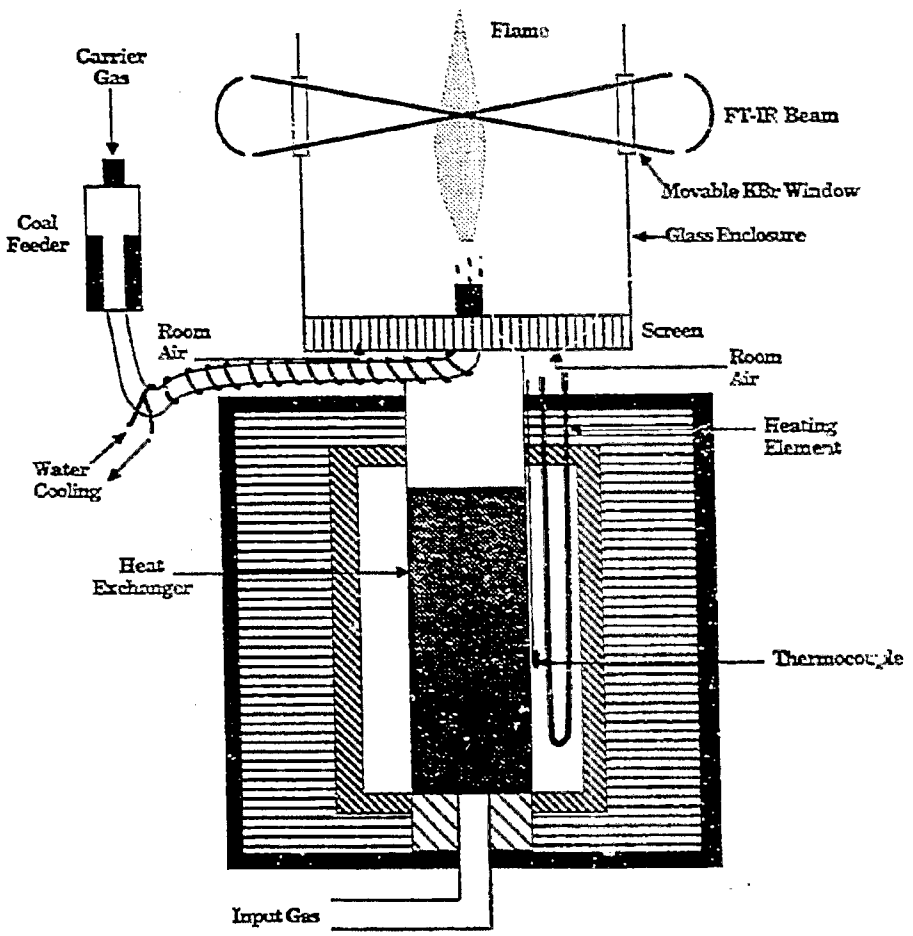


**Figure 1.** Transparent Wall Reactor.

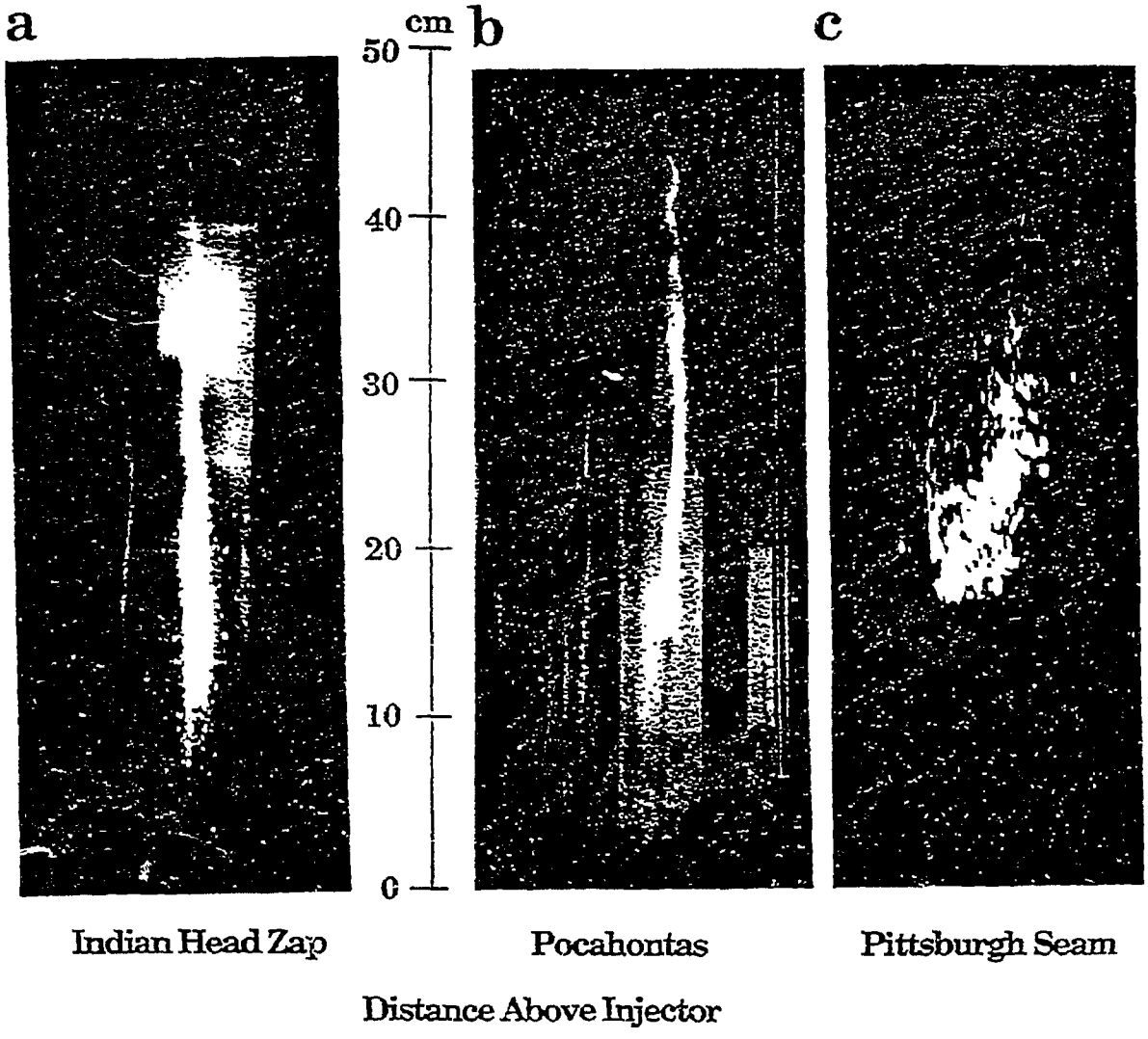


Figure 2. Photographs of a) Zap North Dakota Lignite Flame and b) a Pocahontas Bituminous Coal Flame. The Scale in the Center is Distance Above the Injector Nozzle. c) is a Close up of a Pittsburgh Seam Bituminous Coal Flame.

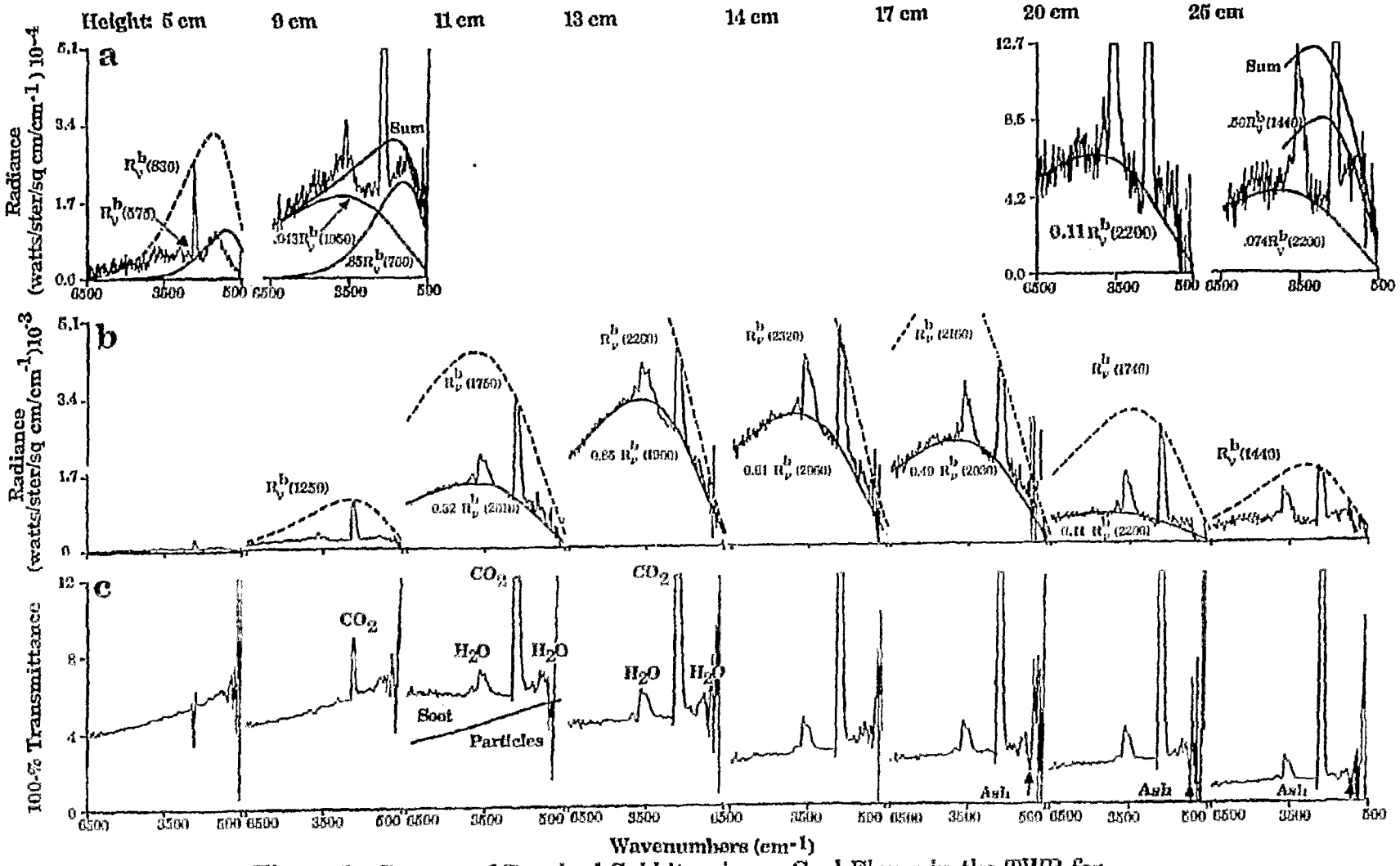


**Figure 3.** Spectra of Rosebud Subbituminous Coal Flame in the TWR for Several Positions Above the Coal Injection Nozzle. a) Normalize Radiance on Expanded Scales, b) Normalized Radiance on a Common Scale, and c) 100 - % Transmittance. The Dashed Lines in a) and b) Represents Black-Body Distributions Fit to the $CO_2$ Band. The Solid Lines in a) and b) Represent Grey-Body Fits to Coal, Char, Ash, and Soot Particles. The Theoretical Black-Body Distributions are Designated as $R_\nu^b(T)$ where T is the Component Temperature is Kelvins.

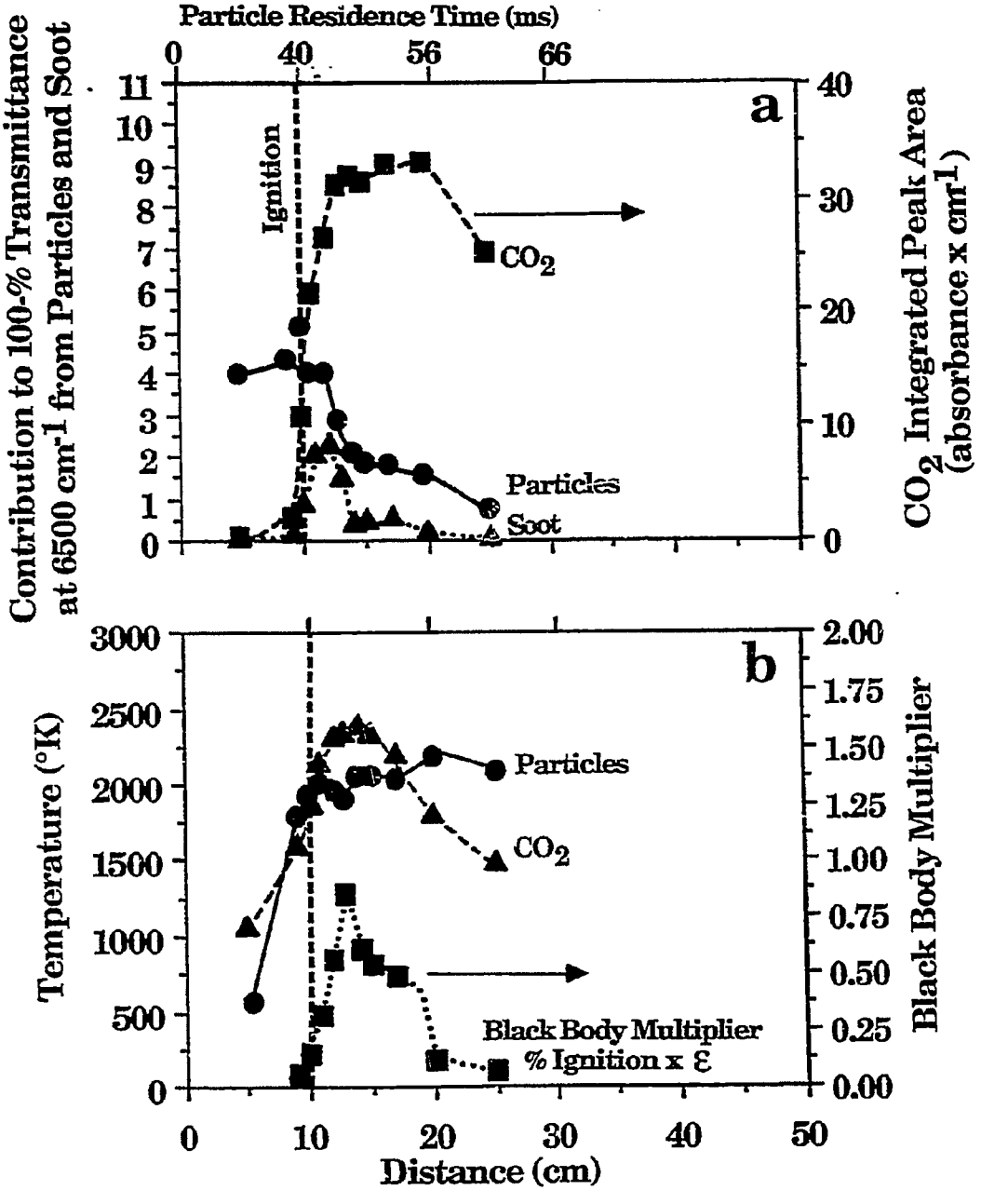


**Figure 4.** Flame Properties as a Function of Distance Above the Injection Nozzle for Montana Rosebud Subbituminous Coal. a) Attenuation from $CO_2$, Particles and Soot and b) Temperature of Particles and $CO_2$ and Fraction of Particles Ignited Times Emissivity.

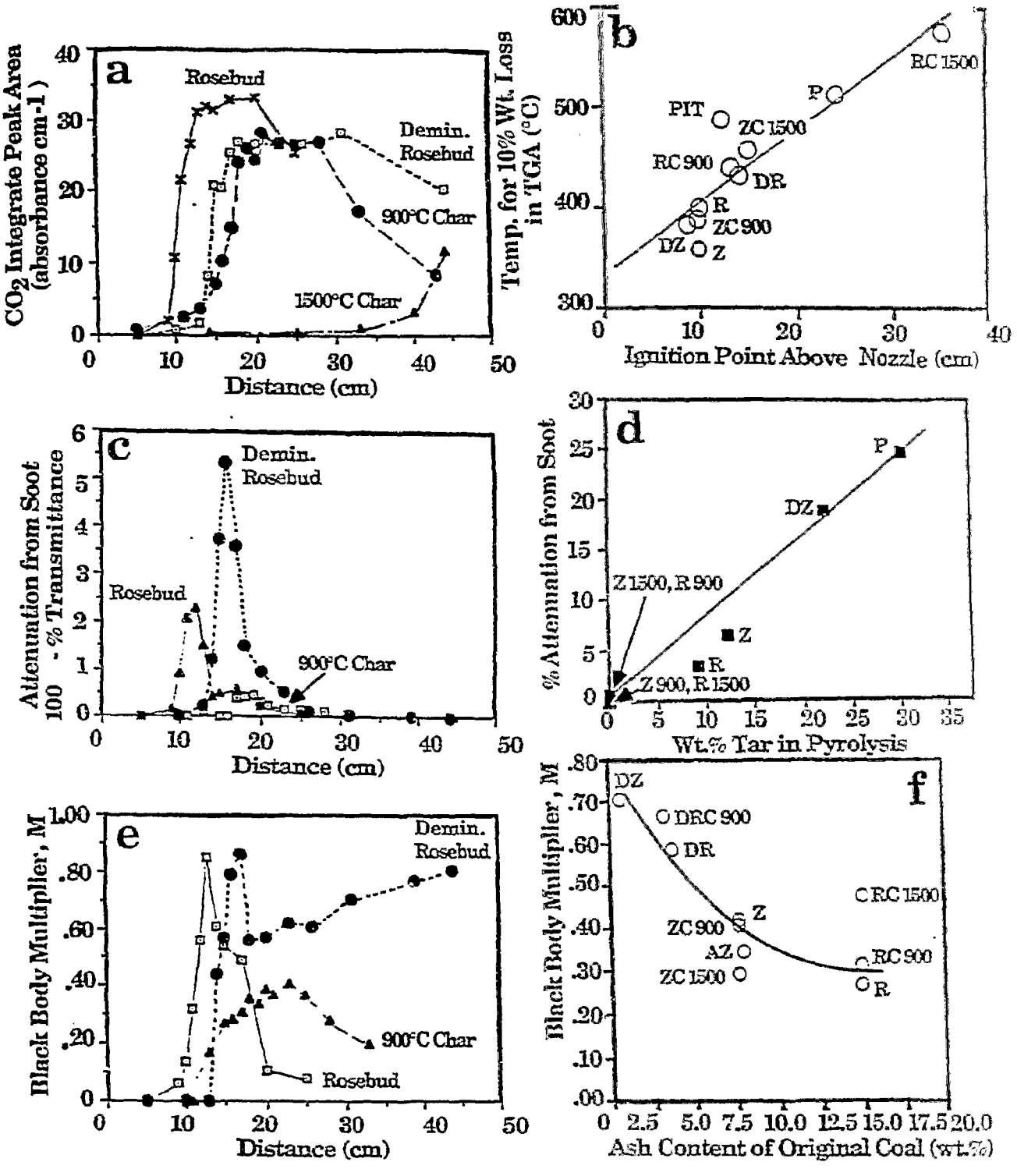


**Figure 5.** Selected Flame Measurements and Correlation of Flame Measurements with Coal Properties. a) Comparison of $CO_2$ Attenuation in Flames of Four Samples, b) Correlation of Ignition Point with TGA Weight Loss in Air, c) Comparison of Soot Attenuation for Three Samples, d) Correlation of Soot Attenuation with Tar Yield in Pyrolysis, e) Comparison of Black Body Multiplier for Three Samples, and F) Correlation of Black Body Multiplier with Ash Content of the Coal.


U.S. DEPARTMENT OF COMMERCE
Technology Administration
National Technical Information Service
Springfield, VA 22161 (703) 605-6000